The du2J mouse model of ataxia and absence epilepsy has deficient cannabinoid CB1 receptor-mediated signalling

Article

Accepted Version

The du^{2J} mouse model of ataxia and absence epilepsy has deficient cannabinoid CB_1 receptor-mediated signalling

Xiaowei Wang, Benjamin J. Whalley* and Gary J. Stephens*

School of Pharmacy, University of Reading, Whiteknights, Reading, RG6 6AJ, UK

*Both authors contributed equally

Running title: Deficient CB_1 signalling in the du^{2J} model

Keywords: cerebellar ataxia, cannabinoid receptor, α2δ subunit

Total number of words: 5470

Corresponding author: Gary J. Stephens, School of Pharmacy, University of Reading, Whiteknights, PO Box 228, Reading RG6 6AJ, UK. E-mail: g.j.stephens@reading.ac.uk

Category: Neuroscience - Cellular/Molecular

Key point summary

- Cerebellar ataxias are progressive debilitating diseases with no known treatment and are associated with defective motor function and, in particular, abnormalities to Purkinje cells.
- Mutant mice with deficits in Ca^{2+} channel auxiliary $\alpha 2\delta$-2 subunits are used as models of cerebellar ataxia.
- Our data in the du^{2J} mouse model shows an association between the ataxic phenotype exhibited by homozygous du^{2J}/du^{2J} mice and increased irregularity of Purkinje cell firing.
- We show that both heterozygous $+/du^{2J}$ and homozygous du^{2J}/du^{2J} mice completely lack the strong presynaptic modulation of neuronal firing by cannabinoid CB_1 receptors which is exhibited by litter-matched control mice.
- These results show that the du^{2J} ataxia model is associated with deficits in CB_1 receptor signalling in the cerebellar cortex, putatively linked with compromised Ca^{2+} channel activity due to reduced $\alpha 2\delta$-2 subunit expression. Knowledge of such deficits may help design therapeutic agents to combat ataxias.

Word count: 147

Abstract

Cerebellar ataxias are a group of progressive, debilitating diseases often associated with abnormal Purkinje cell (PC) firing and/or degeneration. Many animal models of cerebellar ataxia display abnormalities in Ca^{2+} channel function. The 'ducky' du^{2J} mouse model of ataxia and absence epilepsy represents a clean knock-out of the auxiliary Ca^{2+} channel subunit, $\alpha 2\delta$-2, and has been associated with deficient Ca^{2+} channel function in the cerebellar cortex. Here, we investigate effects of du^{2J} mutation on PC layer (PCL) and granule cell (GC) layer (GCL) neuronal spiking activity and, also, inhibitory neurotransmission at interneurone-Purkinje cell (IN-PC) synapses. Increased neuronal firing irregularity was seen in the PCL and, to a less marked extent, in the GCL in du^{2J}/du^{2J}, but not $+/du^{2J}$, mice; these data suggest that the ataxic phenotype is associated with lack of precision of PC firing, that may also impinge on GC activity and requires expression of two du^{2J} alleles to manifest fully. du^{2J} mutation had no clear effect on spontaneous inhibitory postsynaptic current (sIPSC) frequency at IN-PC synapses, but was associated with increased sIPSC amplitudes. du^{2J} mutation ablated cannabinoid CB_1 receptor (CB_1R)-mediated modulation of spontaneous neuronal spike firing and CB_1R-mediated presynaptic inhibition of synaptic transmission at IN-PC synapses in both $+/du^{2J}$ and du^{2J}/du^{2J} mutants; effects that occurred in the absence of changes in CB_1R expression. These results demonstrate that the du^{2J} ataxia model is associated with deficient CB_1R signalling in the cerebellar cortex, putatively linked with compromised Ca^{2+} channel activity and the ataxic phenotype.

Abbreviations

CV, coefficient of variation; GPCR, G protein-coupled receptor; GC, granule cell; GCL, granule cell layer; IN-PC; interneurone-Purkinje cell, ISI, inter-spike interval; MWU, Mann-Whitney U test; PC, Purkinje cell; PCL, Purkinje cell layer; WIN55,212-2; WIN55

Introduction

Cerebellar ataxias comprise a group of progressive diseases associated with motor incoordination and are typically associated with dysfunction and/or degeneration of PCs, which represent the sole efferent output of the cerebellar cortex. A number of mutant mouse models exhibit specific ataxias with diverse behavioural phenotypes at different developmental stages (Green, 1981; Grüsser-Cornehls & Baurle, 2001), including the du^{2J} mutation that exhibits behavioural traits consistent with cerebellar ataxia and absence epilepsy. du^{2J} mice have mutations in the Cacna2d2 gene which encodes the α2δ-2 auxiliary Ca^{2+} channel subunit (Donato *et al*., 2006); one of four α2δ subunit isoforms (α2δ-1-4) that exert auxiliary effects on Ca^{2+} channel biophysical properties and physiological function (Gao *et al*., 2000; Hobom *et al*., 2000; Klugbauer *et al*., 2003; Bauer *et al*., 2010; Dolphin, 2012; Hoppa *et al*., 2012). du^{2J} mice are part of a group of mutant mouse strains together with either spontaneous ($Cacna2d2^{entla}$ and $Cacna2d2^{du}$ alleles) or targeted ($Cacna2d2^{tm1NCIF}$) α2δ-2 disruptions, all of which typically exhibit smaller than normal size, comparable ataxia phenotypes, absence seizures and paroxysmal dyskinesia (Barclay *et al*., 2001; Brodbeck *et al*., 2002; Inanov *et al*., 2004; Brill *et al*., 2004; Donato *et al*., 2006; Walter *et al*., 2006). The $Cacna2d2^{entla}$ allele predicts a full-length protein with an inserted region in the α2 moiety of α2δ-2 and is associated with reduced PC Ca^{2+} currents (Brill *et al*., 2004). The $Cacna2d2^{du}$ allele disrupts Cacna2d2 in intron 3, yielding a truncated α2δ-2 protein and resulting in reduced native and recombinant $Ca_V2.1$ Ca^{2+} channel expression (Barclay *et al*., 2001; Brodbeck *et al*., 2002). The $Cacna2d2^{du2J}$ allele used here has a 2 bp deletion in exon 9 of Cacna2d2 resulting in complete ablation of α2δ-2 expression and reduced PC Ca^{2+} currents (Donato *et al*., 2006). In du mutant mice, a reduction in Ca^{2+} influx, leading to compromised Ca^{2+}-dependent K^+ channel (SK) activity and irregular pacemaking, was proposed to underlie the ataxic phenotype (Walter *et al*., 2006); similarly, the du^{2J} mutation exhibits increased PC

firing irregularity, although this could not be normalised using SK blockers (Donato *et al*., 2006).

Here, we extend previous studies to examine the effect of du^{2J} mutation on basal neuronal network activity and synaptic transmission and, further, on G protein-coupled receptor (GPCR)-mediated presynaptic inhibition of synaptic transmission in the cerebellum. In particular, CB_1 GPCRs are strongly expressed in the cerebellar cortex, where they modulate GABA transmission at IN-PC synapses to modulate PC total output (Ma *et al*., 2008; Wang *et al*., 2011). We demonstrate that the du^{2J} phenotype exhibits deficient CB_1R signalling at the neuronal network level that reflects, at least in part, ablation of CB_1R modulation of inhibitory neurotransmission at IN-PC synapses, but which does not result from reduced CB_1R expression. These results suggest that α2δ-2 deficits in du^{2J} mutants affect GPCR-mediated modulation of inhibitory transmission in the cerebellar cortex, with consequential effects upon PC spike firing activity; such deficits may be associated with ataxic phenotypes and, potentially, contribute to disease.

Methods

Ethical approval

All work was subject to Local Ethical Research Panel approval and was conducted in accordance with the UK Animals (Scientific Procedures) Act, 1986; every effort was made to minimise pain and discomfort experienced by animals.

Electrophysiology

Preparation of acute cerebellar slices. Breeding pairs of +/du^{2J} mice (C57Bl/6 background) were originally supplied by Prof. Annette Dolphin (University College London, UK) from which progeny were bred in-house at the University of Reading and whose genetic classification was determined by the Sequencing & Genotyping Facility, University College London from ear-notch tissue samples. Acute cerebellar brain slices were prepared from 3-5 week old male mice as previously described (Ma *et al.*, 2008). Briefly, animals were sacrificed by a Schedule 1 method followed by immediate decapitation. The brain was then rapidly removed and submerged in cold, sucrose-based aCSF solution (sucrose 218 mM, KCl 3 mM, $NaHCO_3$ 26 mM, NaH_2PO_4 2.5 mM, $MgSO_4$ 2 mM, $CaCl_2$ 2 mM and D-glucose 10 mM) and 300 μm thick parasagittal cerebellar slices were prepared using a Vibroslice 725M (Campden Instruments Ltd, UK) or a Vibratome (R. & L. Slaughter, Upminster, UK). Slices were maintained under carboxygenated (95% O_2/5% CO_2), standard aCSF (NaCl 124 mM, KCl 3 mM, $NaHCO_3$ 26 mM, NaH_2PO_4 2.5 mM, $MgSO_4$ 2 mM, $CaCl_2$ 2 mM and D-glucose 10 mM) at 37°C for <1 h before being returned to room temperature (22-24°C). Recordings were made at 22-24°C, 2-8 h following slice preparation.

Multi-electrode array (MEA) recording. Spontaneous unit and multi-unit spikes were recorded from acute cerebellar slices with respect to a reference ground electrode using

substrate integrated MEAs (Multi Channel Systems, Reutlingen, Germany) that consisted of 59 recording electrodes (30 μm diameter; 200 μm spacing) arranged in an 8×8 matrix minus corner electrodes as previously described (Ma *et al*., 2008). Briefly, slices were adhered to the MEA surface and imaged via a Mikro-Okular camera (Bresser, Germany); once placed, the slice was submerged in carboxygenated standard aCSF, maintained at 24^{o}C and perfused at a rate of ~2 ml/min and allowed to equilibrate for at least 15 min prior to recordings. Signals were amplified (1100× gain) and high-pass filtered (10 Hz) by a 60-channel amplifier (MEA60 System, MultiChannel Systems, Reutlingen, Germany) and each channel simultaneously sampled at 10 kHz. Continuous recordings from each channel were made using MC_Rack software (MultiChannel Systems) where control spontaneous neuronal activity was first recorded for ≥10 min. **In all experiments, each drug was bath-applied for ≥25 min to achieve steady-state effects before 300 s duration continuous recordings were taken. Spike events within continuous recordings were identified using MC_Rack by threshold detection at 4.5x the standard deviation of the mean of a signal-free recording. All analyses included all detected spike events that occurred during the 300 s recording period. Individual spike timings were defined by the time at which the peak minimum for each spike occurred. Spike cut outs were taken for the period 1 ms prior to and 2 ms following each spike's peak minimum (Figure 1Ai). Spike timings were exported to Neuroexplorer4 (Nex Technologies, USA) for analysis of spike firing rates. Mean spike amplitudes were determined from spike cutout data analysed using in-house code for MATLAB 7.1 (MathWorks, Natick, MA, USA).** Regularity of firing was estimated using the coefficient of variation (CV) of interspike interval (ISI), where CV = standard deviation/mean and increases in CV reflect increases in firing irregularity. MEAs have previously been shown to be well suited to recording single unit activity from acute, cerebellar slices (Egert et al., 2002); the validity of such recordings was routinely confirmed

via per electrode autocorrelograms that reliably revealed troughs at t=0 s in PCs, indicative of single units. **Stated replicates undertaken in MEA experiments represent the mean of electrodes for a given cellular population per slice as our unit measurement. Thus, for each slice, measured parameters (firing frequency, spike amplitude, CV) from a particular cell type were calculated for each electrode before averaging to provide a single value per cell type for a given slice. To avoid sampling bias, ≥6 separate slices were used for each treatment group. These data were normally distributed (P<0.05, D'Agostino and Pearson omnibus normality test).** Given the slice-to-slice variability in activity under control conditions, drug effects were normalised by expression of change versus the starting control for each slice. Comparisons between raw measures obtained from wild-type +/+, +/du^{2J} and du^{2J}/du^{2J} mice were performed using one-way analysis of variance followed by Tukey's HSD test or Kruskal-Wallace with Dunn's post hoc test as appropriate. Comparisons between multiple treatment groups were performed using Friedman's followed by Dunn's post hoc test. Throughout, all data are expressed as mean ± SEM unless stated and differences considered significant if P≤0.05.

Patch-clamp recording. Individual cerebellar brain slices were placed in a recording chamber maintained at room temperature and superfused with carboxygenated standard aCSF. PCs were identified morphologically using an IR-DIC upright Olympus BX50WI microscope (Olympus, Tokyo, Japan) with a 60× numerical aperture 0.9, water immersion lens. Whole-cell patch-clamp recordings from PCs were made in voltage clamp mode with an EPC-9 patch-clamp amplifier (HEKA Electronik, Lambrecht, Germany) using Pulse software (HEKA) on a Macintosh G4 computer (Apple Computer, Cupertino, CA). Electrodes were fabricated from borosilicate glass (GC150-F10, Harvard Apparatus, Kent, UK) and had resistances ~5-7 MΩ when filled with an intracellular solution (CsCl 140 mM, $MgCl_2$ 1 mM,

$CaCl_2$ 1 mM, EGTA 10 mM, MgATP 4 mM, NaGTP 0.4 mM and HEPES 10 mM, pH 7.3). Series resistance was measured at 15-20 MΩ with 70-90% compensation. sIPSCs were isolated at IN-PC synapses in the presence of the non-selective ionotropic glutamate receptor antagonist, NBQX (5 μM), at a holding potential of -70 mV (Stephens *et al*., 2001). Data were sampled at 5 kHz and filtered at one-third of the sampling frequency. Drugs were diluted in aCSF and superfused ≥25 min and at least 150 s recording obtained during the steady-state period was used as raw data for event detection.

Data were initially exported using Pulsefit (HEKA) to AxoGraph 4.0 software for event detection using a sliding template function. Data were normally distributed ($P<0.05$, D'Agostino and Pearson omnibus normality test). Comparisons between measures obtained from +/+, +/du^{2J} and du^{2J} /du^{2J} mice were performed using a one-way ANOVA test followed by Tukey's HSD test. Comparison of multiple treatment groups was performed using repeated measurement one-way ANOVA, followed by Tukey's HSD test.

Radioligand binding assays

Membrane preparation

Cerebellar tissue was dissected from +/+, +/du^{2J} or du^{2J} mice (3-5 week old, male) and stored separately at -80°C until use, as previously described (Jones *et al*., 2010). Tissue was suspended in a membrane buffer containing Tris-HCl 50 mM, $MgCl_2$ 5 mM, EDTA 2 mM and 0.5 mg/ml fatty acid-free BSA and complete protease inhibitor (pH 7.4, Sigma, UK) and subsequently homogenised using an Ultra-Turrax blender (IKA, UK). Homogenates were centrifuged at 1200 g for 10 min and supernatants decanted. Resulting pellets were homogenised and centrifugation repeated. Pooled supernatants were then centrifuged at 39000 g for 30 min in a high-speed centrifuge (Sorvall, UK) and supernatants discarded. Remaining pellets were resuspended in membrane buffer and protein content determined by

Lowry assay (Lowry *et al*., 1951).

Saturation binding assay. An initial saturation binding assay was carried out using increasing concentrations of the tritiated CB_1R antagonist, [^{3}H]SR141716A; the CB_1R antagonist, AM251, was used as the non-specific competitor (as previously described in Jones *et al*., 2010). All concentrations tested were performed in triplicate in assay buffer (20 mM HEPES, 1 mM EDTA, 1 mM EGTA, 0.5%$^w/_v$ fatty acid-free BSA, pH 7.4). All drug stocks and membrane preparations were diluted in assay buffer and stored on ice immediately prior to use. Assay tubes contained a final volume of 1 ml with [^{3}H]SR141716A to final concentrations of (nM): 0.1, 0.2, 0.5, 1, 2, 5, 10, 20 and a final concentration of 10 μM AM251 to determine non-specific binding. Assays were initiated by addition of 30 μg membrane protein and were incubated for 1.5 h at 25°C for ligands to reach equilibrium and terminated by rapid filtration through Whatman GF/C filters using a Brandell cell harvester. This was followed by 4 washes with 3 ml ice-cold PBS (0.14 M NaCl, 3 mM KCl, 1.5 mM KH_2PO_4, 5 mM Na_2HPO_4; pH 7.4) to remove unbound radioactivity. Filters were soaked in 2 ml scintillation fluid overnight. Radioactivity was quantified by liquid scintillation spectrometry using a Wallac 1414 scintillation counter where radioactivity bound to cerebellar membrane was quantified in DPM before conversion to pmol/mg.

Analyses of saturation binding assay data were conducted by non-linear regression and fitted to a one-binding site model (Jones *et al*., 2010) to determine the equilibrium dissociation constant K_d (nM) and maximal number of binding sites B_{max} (pmol/mg) using GraphPad Prism software (version 4.03; GraphPad Software Inc., San Diego, CA). One-way ANOVA was used to compare results obtained from +/+, +/du^{2J} and du^{2J}/du^{2J} mouse tissues, followed by Tukey's HSD test when appropriate.

Pharmacology

NBQX, WIN55,212-2 (WIN55; each made up as 1000x stocks) and AM251 (made up as a 5000x stock) were dissolved in DMSO and stored at -20°C. Drug stock solutions were diluted to final desired bath concentration using carboxygenated standard aCSF immediately before application.

Results

We have investigated the effects of du^{2J} mutation on cerebellar function by comparing +/+ wild-type litter-matched controls with heterozygous +/du^{2J}, which have >50% reduction in α2δ-2 protein (Donato *et al*., 2006), and du^{2J}/du^{2J} mice, which exhibit complete α2δ-2 ablation, reduced whole-cell PC Ca^{2+} current, an ataxic phenotype and fail to survive to adulthood (Donato *et al*., 2006).

du^{2J} mutation affects spontaneous neuronal spike activity in the cerebellum

The cerebellum consists of the PCL, whose principal PC cells represent the sole output of the cerebellar cortex, the GCL and the molecular layer that, together, provide a well-defined architecture for acute brain slice investigations of spatio-temporal network activity using multi-electrode methods (Egert *et al*., 2002; Ma *et al*., 2008). Within the PCL, du^{2J} mutation significantly increased spike firing irregularity in du^{2J}/du^{2J} compared with +/+ and +/du^{2J} (both $P<0.001$; Fig. 1Aiv); PCL spike firing frequency (Fig. 1Aii) and spike amplitude (Fig. 1Aiii) were unaffected. Within the GCL, du^{2J}/du^{2J} exhibited significantly more irregular firing compared to either +/+ or +/du^{2J} (both $P<0.01$; Fig. 1Biv), with no genotype-specific difference in firing frequency (Fig. 1Bii) or spike amplitude (Fig. 1Biii). Overall, these initial results reveal changes in spontaneous network firing properties resulting from du^{2J} mutation that most clearly manifest as globally increased PCL firing irregularity in homozygous du^{2J}/du^{2J} mice, and suggest that the major effect of du^{2J} mutation was to reduce cerebellar PC firing precision, potentially with secondary effects on GCL firing, an effect requiring two du^{2J} alleles to manifest fully.

du^{2J} mutation attenuates CB_1R modulation of spontaneous neuronal spike activity in the cerebellum

CB_1Rs are highly expressed in the cerebellum (Tsou *et al*., 1997), where they strongly regulate PC network activity and, consequentially, modulate the final output of the cerebellar cortex (Ma *et al*., 2008). Modulation of CB_1R function can cause severe motor incoordination (including ataxia), as associated with cerebellar dysfunction (DeSanty & Dar, 2001; Patel & Hillard, 2001). CB_1R modulation has been suggested as a precipitating factor for cerebellar ataxias (Smith & Dar, 2006). Therefore, we next examined CB_1R ligand effects upon spontaneous neuronal activity in cerebellar slices from +/+, +/du^{2J} and du^{2J}/du^{2J} mice. We first recapitulated our previous study (performed in TO strain mice, Ma *et al*., 2008) to confirm that the CB_1R agonist, WIN55 (5 μM), significantly increased PCL spike firing frequency ($P<0.05$ vs control), an action fully reversed by subsequent application of CB_1R antagonist, AM251 (2 μM), in the continued presence of WIN55 in +/+ ($P<0.01$ vs WIN55 only; Fig. 2Ai,ii). In these experiments, neither WIN55 nor AM251 affected PCL spike amplitude (Fig. 2Aiii) or spike firing regularity (Fig. 2Aiv). We next investigated whether du^{2J} mutation consequentially affected CB_1R-mediated modulation of PC firing. Importantly, WIN55 (5 μM) and AM251 (2 μM) failed to affect PCL spike firing frequency, spike amplitude or regularity of firing in +/du^{2J} (Fig. 2Bi-iv) or du^{2J}/du^{2J} (Fig. 2Ci-iv).

We next examined CB_1R ligand effects on GCL spontaneous spike firing in the du^{2J} genotypes. In +/+, WIN55 (5 μM) and subsequent AM251 (2 μM) application in the continued presence of WIN55 had no effect on GCL firing frequency (Fig. 3Ai,ii), spike amplitude (Fig. 3Aiii) or firing regularity (Fig. 3Aiv). Similarly, WIN55 and AM251 did not affect GCL spike firing in +/du^{2J} (Fig. 3Bi-iv) or du^{2J}/du^{2J} (Fig. 3Ci-iv). These results most likely reflect the reported lack of CB_1R expression in GC neurones (Tsou *et al*., 1997; Egertova & Elphick, 2000). Overall, these findings show that that CB_1R ligands predictably modulate cerebellar PCL network level activity in +/+, but not +/du^{2J} or du^{2J}/du^{2J}, and are without effect on GCL firing, independent of genotype.

du^{2J} mutation affects CB_1R-mediated presynaptic inhibition at inhibitory IN-PC synapses

We have previously shown that PC firing can be affected by CB_1R-mediated modulation of presynaptic GABA release at IN-PC synapses (Ma *et al*., 2008). Given our data showing that CB_1R-modulation of spontaneous neuronal firing is absent in du^{2J} mutants, we next investigated whether du^{2J} mutation affected CB_1R modulation of inhibitory transmission at IN-PC synapses. Presynaptic Ca^{2+} channels (predominantly $Ca_V2.1$) underlie GABA release at IN-PC synapses (Forti *et al*., 2000; Stephens *et al*., 2001; Lonchamp *et al*., 2009) and the du^{2J} mutation has been shown to impair PC Ca^{2+} channel function (Donato *et al*., 2006). Therefore, we recorded sIPSCs to allow us to determine the effects of du^{2J} mutation on action potential-induced, Ca^{2+}-mediated vesicular neurotransmitter release (Stephens *et al*., 2001) and, also, to investigate potential associations between effects at IN-PC synapses and the action potential-dependent spontaneous PC spike firing measurements described above. No significant differences in sIPSC frequency (Fig. 4A,Bi) or regularity (Fig. 4A,Biii) between +/+, +/du^{2J} and du^{2J}/du^{2J} were observed, although +/du^{2J} and du^{2J}/du^{2J} each exhibited significantly increased sIPSC amplitudes when compared with +/+ (+/du^{2J}: $P<0.05$; du^{2J}/du^{2J}: $P<0.01$; Fig. 4Bii).

We next confirmed the predicted CB_1R modulation of sIPSC frequency at +/+ IN-PC synapses (Takahashi & Linden, 2001; Szabo *et al*., 2004). Thus, WIN55 (5 μM) significantly decreased sIPSC frequency ($P<0.05$), an effect that was reversed and increased beyond control levels by subsequent AM251 (2 μM) application in +/+ ($P<0.01$; Fig. 5Ai,ii). The latter result is consistent with the presence of endocannabinergic tone or constitutive CB_1R activity in this system (Ma *et al*., 2008; Wang *et al*., 2011). Consistent with the lack of CB_1R-mediated effects on neuronal spiking activity described above, WIN55 and AM251 failed to significantly modulate sIPSC frequency in +/du^{2J} (Fig. 5Bi,ii) or du^{2J}/du^{2J} (Fig. 5Ci,ii),

although both WIN55 and AM251 showed a marginal trend (P=0.07; repeated measurement one-way ANOVA) to modulate sIPSC frequency in +/du^{2J} (Fig. 5Bii) not seen in du^{2J}/du^{2J} (P=0.19; Fig. 5Cii). In addition, WIN55 significantly increased sIPSC amplitude in +/+ (P<0.05; Fig. 5Aiii) and +/du^{2J} (P<0.05; Fig. 5Biii), but not du^{2J}/du^{2J} (P=0.11; Fig. 5Cii). Subsequent AM251 application was without effect on WIN55-induced increases in sIPSC amplitude in +/+ (Fig. 5Aiii) and +/du^{2J} (Fig. 5Biii). The inability of AM251 to block WIN55-induced increases in sIPSC amplitude suggests a CB_1R-independent action here.

Taken together, these results demonstrate an attenuation of CB_1R modulation at IN-PC synapses in du^{2J} mutants, such effects could contribute to the observed deficits in network level neuronal function.

Investigation of CB1 receptor expression in du^{2J} mice using [^{3}H]SR141716A saturation binding assay

The data above demonstrate that du^{2J} mutants exhibit deficits in CB_1R-mediated signalling in the cerebellum. Such deficits could occur as a consequence of reported defects in α2δ-2 Ca^{2+} channel subunit expression (Donato *et al.*, 2006); however, an alternative hypothesis is reduced CB_1R expression in the cerebella of du^{2J} mutants. To further investigate the latter hypothesis, CB_1R expression was investigated using radioligand saturation binding assays. In +/+, +/du^{2J} and du^{2J}/du^{2J} mice, specific binding of the high-affinity CB_1R antagonist, [^{3}H]SR141716A, to cerebellar membranes was concentration-dependent and saturable (Fig. 6). There was no significant difference in K_d between +/+, +/du^{2J} and du^{2J}/du^{2J} (P=0.47; Table 1) and the Hill coefficient (nH, the gradient of the Hill plot) approximated unity for all genotypes (Table 1), indicating that [^{3}H]SR141716A bound at a single site to cerebellar CB_1Rs. Most importantly, cerebellar membranes from +/+, +/du^{2J} and du^{2J}/du^{2J} mice exhibited no significant differences in B_{max} (P=0.3; Table 1), indicating that there was no

difference in CB_1R expression between genotypes investigated. These data demonstrate that the reported deficit in CB_1R signalling in du^{2J} mutants was likely not to be due to reduced CB_1R expression and, rather, may reflect defects in $\alpha 2\delta$-2 expression, as discussed below.

Discussion

α2δ-2 mouse mutants exhibit ataxia. Here, we use the du^{2J} mutation, a reportedly clean α2δ-2 knockout (Donato *et al*., 2006) permitting clear interpretation of phenotypic differences. In addition to studying homozygous du^{2J}/du^{2J}, we also examine heterozygous $+/du^{2J}$ to investigate potential progressive disturbances. We demonstrate that du^{2J} mutants exhibit deficits in cerebellar CB_1R-mediated signalling.

Effects of du^{2J} mutation on neuronal spike activity in the cerebellum

PCL and GCL spike firing showed negative polarity (Ma *et al*. 2008; Egert *et al*. 2002). PCL spikes on a given electrode arose from single cells as supported by characteristic trough autocorrelograms and single distribution ISI histograms (data not shown). Conversely, GCL spikes produced variable distribution ISI histograms and autocorrelograms that suggested multi-cell signals (data not shown), accountable for by larger cell somata diameters in PCL than GCL (Egert *et al*., 2002). GCL spike recordings using MEAs show some differences in the literature, ranging from reports of regular activity consistent with the present findings (Egert et al., 2002) to recordings that are '*usually silent*' and where sparse spontaneous activity seen was attributed to Golgi cell activity (Mapelli & D'Angelo, 2007). However, care should be taken when making comparisons between reports where experimental conditions vary (e.g. recordings made at 22-24^{o}C here and in Egert *et al*. (2002) *vs* 32^{o}C in Mapelli & D'Angelo (2007) and can have a profound effect upon basic firing properties. The above caveats for GCL notwithstanding, the major effect of the du^{2J} mutation was to increase PCL irregularity without affecting firing frequency or spike amplitude. du^{2J}/du^{2J}, but not $+/du^{2J}$, exhibited increased PC firing irregularity suggesting progressive dysfunction; this effect could be coupled to differential reduction of α2δ-2 protein expression between $+/du^{2J}$ and du^{2J}/du^{2J} (50% vs 100% respectively, Donato *et al*., 2006)**.** We confirm that expression of two

du^{2J} alleles is required for manifestation of increased PC irregularity and an ataxic phenotype. Although du^{2J} cerebella are smaller than +/+, du^{2J} mutants show no differences in dendritic morphology (Donato *et al*., 2006), arguing against PC degeneration underlying differences in firing regularity. Both PC firing precision and activity patterns play important roles in cerebellar motor control (Womack & Khodakhah, 2002, De Zeeuw *et al*., 2011), potentially by time-locking PC spiking activity (Person & Raman, 2012). Such precision is affected by behavioural state and tactile stimulation (Shin *et al*., 2007). Importantly, many Ca^{2+} channel mutants, including du and du^{2J}, increase PC firing irregularity (Hoebeek *et al*., 2005; Donato *et al*., 2006; Walter *et al*., 2006; Ovsepian & Friel, 2010; Alviña & Khodakhah, 2010), predicted to adversely affect cerebellar function; for example, PC firing irregularity in *tottering* mutants functionally reduces compensatory eye movement amplitude (Hoebeek *et al*., 2005). Donato *et al*. (2006) reported reduced spontaneous PC firing frequency in $+/du^{2J}$ that was further reduced in du^{2J}/du^{2J}, although this was not observed here or in studies using du mutants (Walter *et al*., 2006). These differences may be developmental, as supported by the younger animals used by Donato *et al*. (2006) in comparison to those used here and by Walter *et al*. (2006); however, it is clear that the major, consistent effect of the du2J mutation is to increase firing irregularity.

It has been proposed that GCL firing, driven by mossy fibre inputs, manifests as precisely timed spike bursts limited by Golgi cell-mediated feedforward inhibition to form discrete time-windows (~5 ms) for control of distinct motor domains; thus GC spike firing dysfunction could contribute to ataxic symptoms (e.g. hypermetria) (D'Angelo & De Zeeuw, 2009). Here, GCL firing irregularity was increased in du^{2J}/du^{2J}, although to a far lesser extent than in PCL. During development, GC survival depends upon connectivity with PCs (Lossi *et al*., 2002) and PC disturbances adversely affected GC (Goldowitz & Hamre, 1998), with PC-dependent GCL degeneration also proposed (Ivanov *et al*., 2004); this phenomenon is also

reported for ataxic *lurcher* mice (Wetts & Herrup, 1982). Interestingly, α2δ-2 subunits are barely expressed in GCL, and GC Ca^{2+} currents were normal in du mutants (Barclay *et al*., 2001; Donato *et al*., 2006), consistent with GC changes reflecting secondary consequences of PC dysfunction. Overall, although connectivity deficiencies between cerebellar layers in du^{2J} mutants remain unproven, our results provide evidence for a role of α2δ-2 in correct PC-GC signalling and suggest that the impact of α2δ-2 loss on the GCL should not be ignored.

Effects of du^{2J} mutation on inhibitory synaptic transmission in the cerebellum

Whilst effects of du^{2J} mutation on synaptic transmission are unknown, ataxic mouse models exhibit differences in excitatory transmission in some studies (Matsushita *et al*., 2002; Liu & Friel, 2008), but not others (Zhou *et al*., 2003); *leaner* mutants exhibit enhanced inhibitory transmission, proposed to underlie reduced PC firing and increased irregularity (Liu & Friel, 2008). In addition to intrinsic properties, tonic inhibitory inputs also regulate PC output and synchronization (Hausser & Clark, 1997; de Solages *et al*., 2008). Here, sIPSC frequencies were unaffected between genotypes, suggesting that action potential-mediated, basal GABA release is unaltered by du^{2J} mutation. **Interestingly, sIPSC amplitude was significantly increased in +/du^{2J} and du^{2J}/du^{2J} (*c.f.* +/+ littermates). A similar increase has been reported for *leaner* mutants and attributed to increased presynaptic GABA release (Ovsepian & Friel, 2012); such effects are unlikely here due to the reported lack of change to sIPSC frequency.** An alternative hypothesis is an increase in postsynaptic $GABA_A$ receptor responsiveness. Increased intracellular Ca^{2+} ($[Ca^{2+}]_i$) can suppress postsynaptic $GABA_A$ receptor function, potentially by decreasing GABA affinity for $GABA_A$ receptors (Inoue *et al*., 1986; Martina *et al*., 1994); therefore, reduced $[Ca^{2+}]_i$, as predicted for decreased PC α2δ-2 expression in du^{2J} mutants (Donato *et al*., 2006), may relieve Ca^{2+}-mediated suppression of $GABA_A$ receptor function.

CB_1R modulation is abolished in du^{2J} mutants

Whilst we found no changes to basal IN-PC inhibitory transmission, it remains possible that du^{2J} mutation disrupts presynaptic regulatory mechanisms, including GPCR-mediated inhibition (Zhou *et al*., 2003). Here, no CB_1R-mediated modulation was seen in $+/du^{2J}$ and du^{2J}/du^{2J}, as demonstrated by an absence of CB_1R agonist-mediated increases in PC spike firing and lack of reductions in inhibitory transmission at IN-PC synapses compared to +/+. These findings suggest that deficits in CB_1R presynaptic inhibition of GABA release is associated with this model of ataxia and could contribute to compromised normal regulation of total PC output and, potentially, the aberrant motor phenotype associated with deficient PC function.

Unlike changes to PC firing regularity, which were confined to homozygous du^{2J}/du^{2J}, heterozygous $+/du^{2J}$ showed CB_1R signalling deficits similar to du^{2J}/du^{2J}. However, WIN55 and AM251 showed a statistical trend to modulate sIPSC frequency in $+/du^{2J}$ mice not seen in du^{2J}/du^{2J}, offering some support to a progressive deficit in modulation of presynaptic inhibition. Somewhat unexpectedly, WIN55 increased sIPSC amplitude in +/+ and $+/du^{2J}$, this increase may reflect a postsynaptic phenomena; in this regard, the lack of AM251-induced reversal of WIN55 effects (Wang *et al*., 2011) suggests that this WIN55 effect is CB_1R-independent, consistent with the reported lack of postsynaptic CB_1R expression (Tsou *et al*., 1997; Yamasaki *et al*., 2006). For example, WIN55 inhibits $Ca_V2.1$ channels in PCs at concentrations used here (Fisyunov *et al*., 2006; Lozovaya *et al*., 2009), such actions could reduce $[Ca^{2+}]_i$ to overcome Ca^{2+}-mediated suppression of $GABA_A$ receptor function (Inoue *et al*., 1986; Martina *et al*., 1994) in +/+ and $+/du^{2J}$; the lack of effect in du^{2J}/du^{2J} may reflect reduced PC Ca^{2+} current levels in homozygotes (Donato *et al*., 2006). Overall, whilst expression of two du^{2J} alleles is required for increased PC irregularity and ataxia, our results

demonstrate that expression of a single du^{2J} allele compromises CB_1R signalling, prior to any measurable change in PC firing regularity and any clear ataxic phenotype. Here, disrupted cannabinergic signalling may represent a useful diagnostic biomarker of early or asymptomatic cerebellar dysfunction.

Consequences of du^{2J} mutation on CB_1R signalling

We show, for the first time, that α2δ-2 deficits caused by du^{2J} mutation are associated with aberrant CB_1R signalling and suggest links between impaired Ca^{2+} channel function and consequential impairment of GPCR-mediated presynaptic inhibition. We also show that CB_1R expression is unchanged in du^{2J} mutants, suggesting that deficiency occurs downstream of receptor activation. α2δ-2 is the major isoform expressed in PCs (Cole *et al.*, 2005) and reduced α2δ-2 expression in du^{2J} affects Ca^{2+} current levels (Donato *et al.*, 2006). Moreover, α2δ-2 is predominantly associated with $Ca_V2.1$ (Barclay *et al.*, 2001), the major $Ca_V\alpha$ subunit mediating presynaptic GABA release at IN-PC synapses (Stephens *et al.*, 2001). Importantly, PC-specific conditional $Ca_V2.1$ knock-out causes cerebellar ataxia (Todorov *et al.*, 2012). The association of α2δ-2/$Ca_V2.1$ subunits suggest that deficits in either subunit could equally cause motor deficits, as supported by similarities in ataxic phenotypes in α2δ-2 mutants, including du^{2J} and $Ca_V2.1$ knockouts. The most parsimonious explanation for our results is that altered α2δ-2 expression in axon terminals of basket and stellate interneurones in du^{2J} mutants leads to deficits in CB_1R-mediated signalling. Although the expression of α2δ-2 in interneurone terminals in cerebellum has not been studied specifically, α2δ-2 is highly expressed in the molecular layer and in GABAergic interneurones throughout the CNS, as well as in PCs (Barclay *et al.*, 2001; Cole *et al.*, 2005). Recent studies have shown that α2δ subunits affect release properties of the Ca^{2+} channel complex at presynaptic terminals by improving spatial coupling between Ca^{2+} influx and exocytosis (Hoppa *et al.*, 2012; Dolphin,

2012), in addition to protecting against block of exocytosis by intracellular Ca^{2+} chelators (Hoppa *et al*., 2012). Such findings are consistent with the hypothesis that proper α2δ-2 expression is required for correct modulation of presynaptic release. Presynaptic CB_1R activation limits transmitter release via generation of Gβγ subunits which inhibit Ca^{2+} channels (Twitchell *et al*. 1997; Stephens, 2009). Here, reduced α2δ-2 in du^{2J} mutants could alter G protein/Ca^{2+} channel interaction to limit direct effects upon channel gating and so dysfunctionally affect modulation of GABA release onto PCs.

Functional impact of CB_1R deficits in cerebellar ataxia

We propose that CB_1R signalling deficits in du^{2J} mutants occur as a consequence of reduced α2δ-2 expression, which impairs Ca^{2+} channel function and affects normal GPCR presynaptic inhibition in ataxic phenotypes. Under normal conditions, CB_1R inhibition of GABA release at IN-PC synapses reduces inhibitory drive onto PCs to increase PC spike firing (Ma *et al*., 2008). Regulation of PC spike firing and regularity modulates activity of deep cerebellar nuclei to control motor function. CB_1R signalling also contributes to presynaptically-expressed synaptic plasticity in the cerebellar cortex. Whilst long-term depression of transmitter release is typically associated with the excitatory parallel fibre (PF)-PC pathway, endocannabinnoid-mediated short term plasticity, in the form of depolarization-induced suppression of inhibition, is prominent at IN-PC synapses (Kano *et al*., 2009). Notably, CB_1R immunoreactivity is reportedly five times higher at IN than at PF terminals; in particular, at basket cell terminals at the PC axon initial segment (Kawamura *et al*., 2006). Therefore, deficits in CB_1R signalling may directly influence PC output in ataxic phenotypes, both in terms of spike firing and regularity, and, also, synaptic function; such deficiencies may contribute to disease.

References

Alviña K & Khodakhah K (2010). K_{Ca} channels as therapeutic agents in episodic ataxia type-2. *J Neurosci* **30**, 7249-7257

Barclay J, Balaguero N, Mione M, Ackerman SL, Letts VA, Brodbeck J, Canti C, Meir A, Page KM, Kusumi K, Perez-Reyes E, Lander ES, Frankel WN, Gardiner RM, Dolphin AC & Rees M (2001). Ducky mouse phenotype of epilepsy and ataxia is associated with mutations in the Cacna2d2 gene and decreased calcium channel current in cerebellar PCs. *J Neurosci* **21**, 6095-6104.

Bauer CS, Tran-Van-Minh A, Kadurin I & Dolphin AC (2010). A new look at calcium channel α2δ subunits. *Curr Opin Neurobiol* **20**, 563-571.

Brill J, Klocke R, Paul D, Boison D, Gouder N, Klugbauer N, Hofmann F, Becker CM & Becker K (2004). entla, a novel epileptic and ataxic Cacna2d2 mutant of the mouse. *J Biol Chem* **279**, 7322-7330.

Brodbeck J, Davies A, Courtney JM, Meir A, Balaguero N, Canti C, Moss FJ, Page KM, Pratt WS, Hunt SP, Barclay J, Rees M & Dolphin AC (2002). The ducky mutation in Cacna2d2 results in altered Purkinje cell morphology and is associated with the expression of a truncated α2δ-2 protein with abnormal function. *J Biol Chem* **277**, 7684-7693.

Cole RL, Lechner SM, Williams ME, Prodanovich P, Bleicher L, Varney MA & Gu G (2005). Differential distribution of voltage-gated calcium channel alpha-2 delta (α2δ) subunit mRNA-containing cells in the rat central nervous system and the dorsal root ganglia. *J Comp*

Neurol **491**, 246-269.

D'Angelo E & De Zeeuw CI (2009). Timing and plasticity in the cerebellum: focus on the granular layer. *Trends Neurosci* **32**, 30-40.

DeSanty KP & Dar MS (2001). Cannabinoid-induced motor incoordination through the cerebellar CB1 receptor in mice. *Pharmacol Biochem Behav* **69**, 251–259.

de Solages C, Szapiro G, Brunel N, Hakim V, Isope P, Buisseret P, Rousseau C, Barbour B & Léna C (2008). High-frequency organization and synchrony of activity in the Purkinje cell layer of the cerebellum. *Neuron* **58**, 775-788.

De Zeeuw CI, Hoebeek FE, Bosman LW, Schonewille M, Witter L & Koekkoek SK (2011). Spatiotemporal firing patterns in the cerebellum. *Nat Rev Neurosci* **12**, 327-344.

Dolphin AC (2012). Calcium channel auxiliary α2δ and β subunits: trafficking and one step beyond. *Nat Rev Neurosci* **13**, 542-555.

Donato R, Page KM, Koch D, Nieto-Rostro M, Foucault I, Davies A, Wilkinson T, Rees M, Edwards FA & Dolphin AC (2006). The ducky^{2J} mutation in Cacna2d2 results in reduced spontaneous Purkinje cell activity and altered gene expression. *J Neurosci* **26**, 12576-12586.

Egert U, Heck D & Aertsen A (2002). Two-dimensional monitoring of spiking networks in acute brain slices. *Exp Brain Res* **142**, 268-274.

Egertova M & Elphick MR (2000). Localization of cannabinoid receptors in the rat brain using antibodies to the intracellular C-terminal tail of CB1. *J Comp Neurol* **422**, 159–171.

Forti L, Pouzat C & Llano I (2000). Action potential-evoked Ca^{2+} signals and calcium channels in axons of developing rat cerebellar interneurones. *J Physiol* 527, 33–48.

Fisyunov A, Tsintsadze V, Min R, Burnashev N & Lozovaya N (2006). Cannabinoids modulate the P-type high-voltage-activated calcium currents in Purkinje neurons. *J Neurophysiol* **96**, 1267-1277.

Gao BN, Sekido Y, Maximov A, Saad M, Forgacs E, Latif F, Wei MH, Lerman M, Lee JH & Perez-Reyes E (2000). Functional properties of a new voltage-dependent calcium channel α2δ auxiliary subunit gene (CACNA2D2). J *Biol Chem* **275**, 12237-12242.

Goldowitz D & Hamre K (1998). The cells and molecules that make a cerebellum. *Trends Neurosci* **21**, 375-382.

Green MC (ed), (1981). Genetic Variants and Strains of Laboratory Mouse. Stuttgart: Gustav Fischer Verlag. ISBN: 0898741520. pp 1-7.

Grüsser-Cornehls U & Baurle J (2001). Mutant mice as a model for cerebellar ataxia. *Prog Neurobiol* **63**, 489–540.

Hausser M & Clark BA (1997). Tonic synaptic inhibition modulates neuronal output pattern and spatiotemporal synaptic integration. *Neuron* **19**, 665-678.

Hobom M, Dai S, Marais E, Lacinova L, Hofmann F & Klugbauer N (2000). Neuronal distribution and functional characterization of the calcium channel α2δ-2 subunit. *Eur J Neurosci* **12**, 1217-1226.

Hoebeek FE, Stahl JS, van Alphen AM, Schonewille M, Luo C, Rutteman M, van den Maagdenberg AM, Molenaar PC, Goossens HH, Frens MA & De Zeeuw CI (2005). Increased noise level of Purkinje cell activities minimizes impact of their modulation during sensorimotor control. *Neuron* **45**, 953–965.

Hoppa MB, Lana B, Margas W, Dolphin AC & Ryan TA (2012). α2δ expression sets presynaptic calcium channel abundance and release probability. *Nature* **486**, 122-125.

Inoue M, Oomura Y, Yakushiji T & Akaike N (1986). Intracellular calcium ions decrease the affinity of the GABA receptor. *Nature* **324**, 156–158.

Ivanov SV, Ward JM, Tessarollo L, McAreavey D, Sachdev V, Fananapazir L, Banks MK, Morris N, Djurickovic D, Devor-Henneman DE, Wei MH, Alvord GW, Gao B, Richardson JA, Minna JD, Rogawski MA & Lerman MI (2004). Cerebellar ataxia, seizures, premature death, and cardiac abnormalities in mice with targeted disruption of the Cacna2d2 gene. *Am J Pathol* **165**, 1007-1018.

Jones NA, Hill AJ, Smith I, Bevan SA, Williams CM, Whalley BJ & Stephens GJ (2010). Cannabidiol displays antiepileptiform and antiseizure properties *in vitro* and *in vivo*. *J*

Pharmacol Exp Ther **332**, 569-577.

Kano M, Ohno-Shosaku T, Hashimotodani Y, Uchigashima M & Watanabe M (2009). Endocannabinoid-mediated control of synaptic transmission. *Physiol Rev* **89**, 309-380.

Kawamura Y, Fukaya M, Maejima T, Yoshida T, Miura E, Watanabe M, Ohno-Shosaku T & Kano M (2006). CB_1 is the major cannabinoid receptor at excitatory presynaptic site in the hippocampus and cerebellum. *J Neurosci* **26**, 2991–3001.

Klugbauer N, Marais E & Hofmann F (2003). Calcium channel α2δ subunits: differential expression, function, and drug binding. *J Bioenerg Biomembr* **35**, 639-647.

Liu S & Friel DD (2008). Impact of the leaner P/Q-type Ca^{2+} channel mutation on excitatory synaptic transmission in cerebellar Purkinje cells. *J Physiol* **586**, 4501-4515.

Lonchamp E, Dupont JL, Doussau F, Shin HS, Poulain B & Bossu JL (2009). Deletion of $Ca_V2.1$(α1A) subunit of Ca^{2+}-channels impairs synaptic GABA and glutamate release in the mouse cerebellar cortex in cultured slices. *Eur J Neurosci* **30**, 2293-2307.

Lossi L, Mioletti S & Merighi A (2002). Synapse-independent and synapse-dependent apoptosis of cerebellar granule cells in postnatal rabbits occur at two subsequent but partly overlapping developmental stages. *Neuroscience* **112**, 509-523.

Lowry OH, Rosebrough NJ, Farr AL & Randall RJ (1951). Protein measurement with the Folin phenol reagent. *J Biol Chem* **193**, 265-275.

Lozovaya N, Min R, Tsintsadze V & Burnashev N (2009). Dual modulation of CNS voltage-gated calcium channels by cannabinoids: Focus on CB_1 receptor-independent effects. *Cell Calcium* **46**, 154-162.

Ma YL, Weston SE, Whalley BJ & Stephens GJ (2008). The phytocannabinoid Δ^9-tetrahydrocannabivarin modulates inhibitory neurotransmission in the cerebellum. *Br J Pharmacol* **154**, 204-215.

Mapelli J & D'Angelo E. (2007). The spatial organization of long-term synaptic plasticity at the input stage of cerebellum. *J Neurosci* **27**, 1285-1296.

Martina M, Kilic G & Cherubini E (1994). The effect of intracellular Ca^{2+} on GABA-activated currents in cerebella granule cells in culture. *J Membr Biol* **142**, 209-216.

Matsushita K, Wakamori M, Rhyu IJ, Arii T, Oda S, Mori Y & Imoto K (2002). Bidirectional alterations in cerebellar synaptic transmission of *tottering* and *rolling* Ca^{2+} channel mutant mice. *J Neurosci* **22**, 4388–4398.

Ovsepian SV & Friel DD (2012). Enhanced synaptic inhibition disrupts the efferent code of cerebellar Purkinje neurons in *leaner* $Ca_V2.1$ Ca^{2+} channel mutant mice. *Cerebellum* **11**, 666-680.

Patel S & Hillard CJ (2001). Cannabinoid CB_1 receptor agonists produce cerebellar dysfunction in mice. *J Pharmacol Exp Ther* **297**, 629-637.

Person AL & Raman IM (2011). Purkinje neuron synchrony elicits time-locked spiking in the cerebellar nuclei. *Nature* **481**, 502-505.

Shin SL, Hoebeek FE, Schonewille M, De Zeeuw CI, Aertsen A & De Schutter E (2007). Regular patterns in cerebellar Purkinje cell simple spike trains. *PLoS One* **2**, e485.

Smith AD & Dar MS (2006). Mouse cerebellar nicotinic-cholinergic receptor modulation of Δ^9-THC ataxia: role of the α4β2 subtype. *Brain Res* **1115**, 16-25.

Stephens GJ (2009). G-protein-coupled-receptor-mediated presynaptic inhibition in the cerebellum. *Trends Pharmacol Sci* **30**, 421-430.

Stephens GJ, Morris NP, Fyffe RE & Robertson B (2001). The Cav2.1/α1A (P/Q-type) voltage-dependent calcium channel mediates inhibitory neurotransmission onto mouse cerebellar Purkinje cells. *Eur J Neurosci* **13**, 1902-1912.

Szabo B, Than M, Thorn D & Wallmichrath I (2004). Analysis of the effects of cannabinoids on synaptic transmission between basket and Purkinje cells in the cerebellar cortex of the rat. *J Pharmacol Exp Ther* **310**, 915-925.

Takahashi KA & Linden DJ (2000). Cannabinoid receptor modulation of synapses received by cerebellar Purkinje cells. *J Neurophysiol* **83**, 1167–1180.

Todorov B, Kros L, Shyti R, Plak P, Haasdijk ED, Raike RS, Frants RR, Hess EJ, Hoebeek FE, De Zeeuw CI & van den Maagdenberg AM (2012). Purkinje cell-specific ablation of $Ca_V2.1$ channels is sufficient to cause cerebellar ataxia in mice. *Cerebellum* **11**, 246-58.

Tsou K, Brown S, Sañudo-Peña MC, Mackie K & Walker JM (1997). Immunohistochemical distribution of cannabinoid CB_1 receptors in the rat central nervous system. *Neuroscience* **83**, 393-411.

Twitchell W, Brown S & Mackie K (1997). Cannabinoids inhibit N- and P/Q-type calcium channels in cultured rat hippocampal neurons *J Neurophysiol* **78**, 43-50.

Walter JT, Alviña K, Womack MD, Chevez C & Khodakhah K (2006). Decreases in the precision of Purkinje cell pacemaking cause cerebellar dysfunction and ataxia. *Nat Neurosci* **9**, 389-397.

Wang X, Horswill JG, Whalley BJ & Stephens GJ (2011). Effects of the allosteric antagonist PSNCBAM-1 on CB_1 receptor modulation in the cerebellum. *Mol Pharm* **79**, 758-767.

Wetts R & Herrup K (1982). Interaction of granule, Purkinje and inferior olivary neurons in lurcher chimeric mice. II. Granule cell death. *Brain Res* **250**, 358-362.

Womack MD & Khodakhah K (2002). Active contribution of dendrites to the tonic and trimodal patterns of activity in cerebellar Purkinje neurons. *J Neurosci* **22**, 10603-10612.

Yamasaki M, Hashimoto K & Kano M (2006). Miniature synaptic events elicited by presynaptic Ca^{2+} rise are selectively suppressed by cannabinoid receptor activation in cerebellar Purkinje cells. *J Neurosci* **26**, 86–95.

Zhou YD, Turner TJ & Dunlap K (2003). Enhanced G protein-dependent modulation of excitatory synaptic transmission in the cerebellum of the Ca^{2+} channel-mutant mouse, *tottering*. *J Physiol* **547**, 497-507.

Author contributions

Conception and design of the experiments: XW, BJW, GJS

Collection, analysis and interpretation of data: XW, BJW, GJS

Drafting the article or revising it critically for important intellectual content: XW, BJW, GJS

All authors approved the final version of the manuscript.

Acknowledgements

We thank Prof. Annette Dolphin for supply of the original +/du^{2J} breeding pairs. Work was supported by an Ataxia UK Postgraduate Fellowship awarded to BJW and GJS that supported XW. XW also received a University of Reading Postgraduate Research Studentship.

Tables

Table 1. [^{3}H]SR141716A saturation binding data for cerebellar membrane in du^{2J} mutants. K_d and B_{max} were obtained from the saturation binding curves plotted between specific binding vs free [^{3}H]SR141716A radioligand concentration. No significant differences in K_d (P=0.47) or B_{max} (P=0.3) were seen; one-way analysis of variance. Hill slope (nH) was obtained from the Hill plot of the data transformed from saturation binding plot.

Genotype	K_d (nM)	B_{max} (pmol/mg)	nH
+/+ (n=3)	3.1 ± 0.2	2.15 ± 0.08	0.99 ± 0.01
+/du^{2J} (n=3)	2.9 ± 0.3	2.34 ± 0.12	0.99 ± 0.02
du^{2J}/du^{2J} (n=4)	2.4 ± 0.3	2.03 ± 0.21	1.01 ± 0.01

Figure legends

Figure 1. Region-specific comparison of basal spontaneous spike firing properties in du^{2J} mutants.

Ai) Sample traces of continuous MEA recording from a single electrode in PCL in +/+ and du^{2J} mutants where inset shows overlay plot of 50 spikes (grey) and mean spike shape (black) from +/+. Summary bar graph of (**Aii**) spike firing frequency, (**Aiii**) spike amplitude and (**Aiv**) coefficient of variation of interspike interval (CV of ISI). du^{2J}/du^{2J} firing was more irregular compared with +/+ and $+/du^{2J}$. **Bi)** Sample traces of continuous MEA recording from a single electrode in GCL in +/+ and du^{2J} mutants where inset shows overlay plot of 50 spikes (grey) and mean spike shape (black) from +/+. Summary bar graph of (**Bii**) spike frequency, (**Biii**) spike amplitude and (**Biv**) CV of ISI. du^{2J}/du^{2J} firing was more irregular compared with +/+ and $+/du^{2J}$. **= P<0.01; ***= P<0.001; Kruskal-Wallis test followed by Dunn's test.

Figure 2. Differential effects of CB_1R ligands on spontaneous PCL spike activity in du^{2J} mutants.

Sample traces of continuous MEA recording from a single electrode in PCL showing effect of WIN55 (5 μM) and subsequent application of AM251 (2 μM) (in the continued presence of 5 μM WIN55) on spontaneous spike firing in (**Ai**) +/+, (**Bi**) $+/du^{2J}$ and (**Ci**) du^{2J}/du^{2J}. Summary bar graph showing that WIN55 significantly increased normalised spike firing frequency and subsequent application of AM251 caused a significant decrease in normalised spike firing frequency in +/+ (**Aii**). By contrast, WIN55 and subsequent application of AM251 had no significant effect on normalised spike firing frequency in (**Bii**) $+/du^{2J}$ or (**Cii**) du^{2J}/du^{2J}. CB_1R ligands had no effect on spike amplitude in (**Aiii**) +/+, (**Biii**) $+/du^{2J}$ or (**Ciii**) du^{2J}/du^{2J} or on

normalised CV of ISI in (**Aiv**) +/+, (**Biv**) +/du^{2J} or (**Civ**) du^{2J}/du^{2J}. *= P<0.05; **= P<0.01; Friedman test followed by Dunn's test.

Figure 3. Lack of effect of CB_1R ligands on spontaneous GCL spike activity in du^{2J} mutants.

Sample traces of continuous MEA recording from a single electrode in GCL showing lack of effect of WIN55 (5 μM) and subsequent application of AM251 (2 μM) (in the continued presence of 5 μM WIN55) on spontaneous spike firing in (**Ai**) +/+, (**Bi**) +/du^{2J} and (**Ci**) du^{2J}/du^{2J}. Summary bar graph showing that CB_1R ligands had no effect on normalised spike firing frequency in (**Aii**) +/+, (**Bii**) +/du^{2J} or (**Cii**) du^{2J}/du^{2J}, or on spike amplitude in (**Aiii**) +/+, (**Biii**) +/du^{2J} or (**Ciii**) du^{2J}/du^{2J}, or on normalised CV of ISI in (**Aiv**) +/+, (**Biv**) +/du^{2J} or (**Civ**) du^{2J}/du^{2J}; as assessed by Friedman test followed by Dunn's test.

Figure 4. Comparison of basal spontaneous inhibitory transmission at IN-PC synapses in du^{2J} mutants.

A) Raw sIPSC traces from representative PCs from +/+, +/du^{2J} and du^{2J}/du^{2J}. Summary bar graph showing that there was no significant differences in (**Bi**) mean sIPSC frequency and (**Biii**) CV of ISI, but that mean sIPSC amplitude was significant increased in +/du^{2J} and du^{2J}/du^{2J} compared to +/+. *= P<0.05; **= P<0.01; one-way analysis of variance followed by Tukey's HSD test.

Figure 5. Differential effects of CB_1R ligands on inhibitory transmission at IN-PC synapses in du^{2J} mutants.

A) Raw sIPSC traces from representative PCs from (**Ai**) +/+, (**Bi**) +/du^{2J} and (**Ci**) du^{2J}/du^{2J} showing effect of WIN55 (5 μM) and subsequent application of AM251 (2 μM) (in the

continued presence of 5 μM WIN55). **B)** Summary bar graph showing that WIN55 significantly reduced and AM251 significantly increased normalised sIPSC frequency in (**Aii**) +/+, but was without effect in (**Bii**) +/du^{2J} or (**Cii**) du^{2J}/du^{2J}. WIN55 significantly increased normalised sIPSC amplitude in (**Aiii**) +/+ and (**Biii**) +/du^{2J}, but was without effect in du^{2J}/du^{2J} (**Ciii**). Subsequent application of AM251 was without effect in each case. *= P<0.05; **= P<0.01; repeated measurement one-way ANOVA followed by Tukey's HSD test.

Figure 6. Saturation binding of [^{3}H]SR141716A to cerebellar membranes in du^{2J} mutants.

Representative saturation binding curve for [^{3}H]SR141716A in cerebellar membranes from (**A**) +/+, (**B**) +/du^{2J} and (**C**) du^{2J}/du^{2J}.

Figure 1. Wang et al

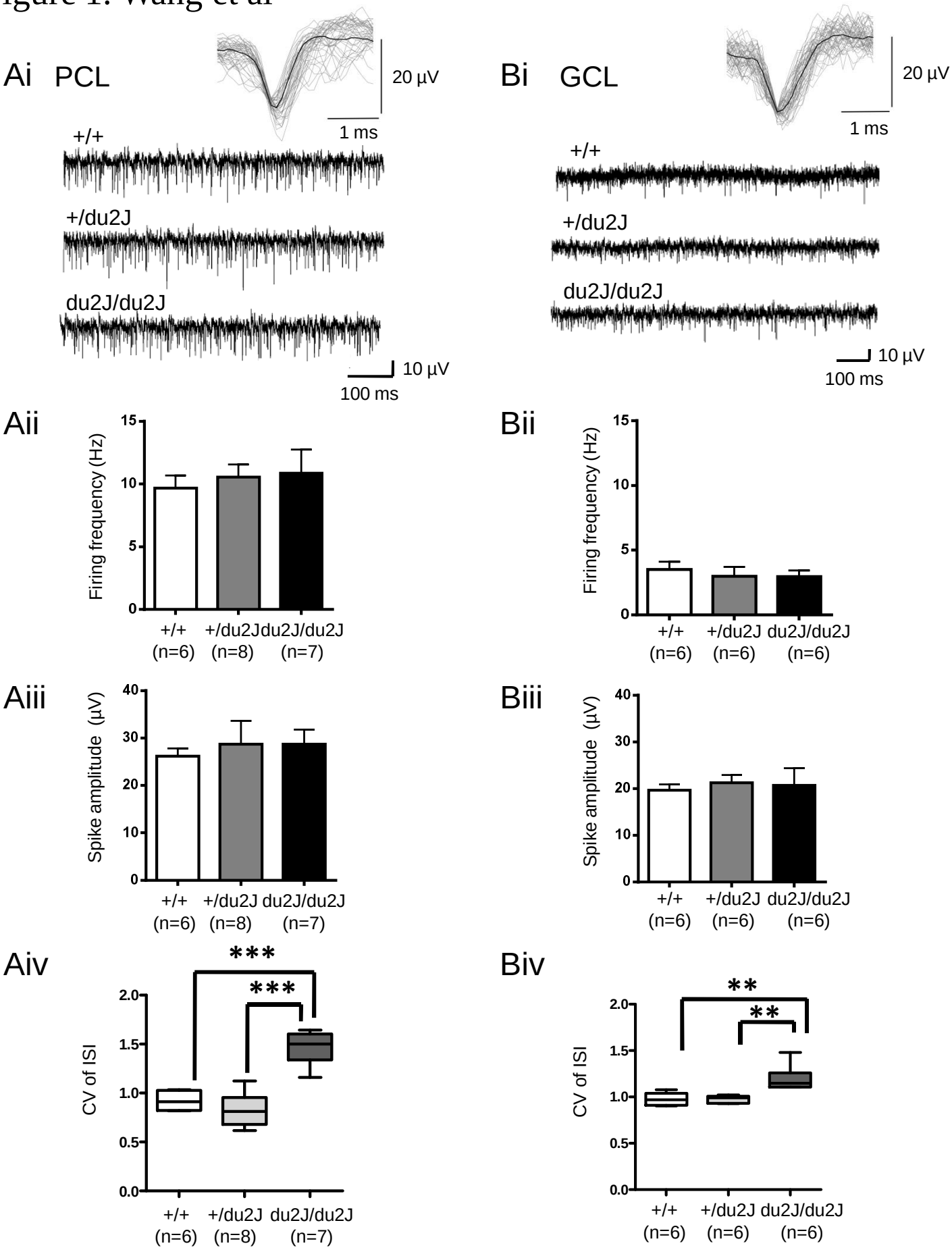

Figure 2. Wang et al

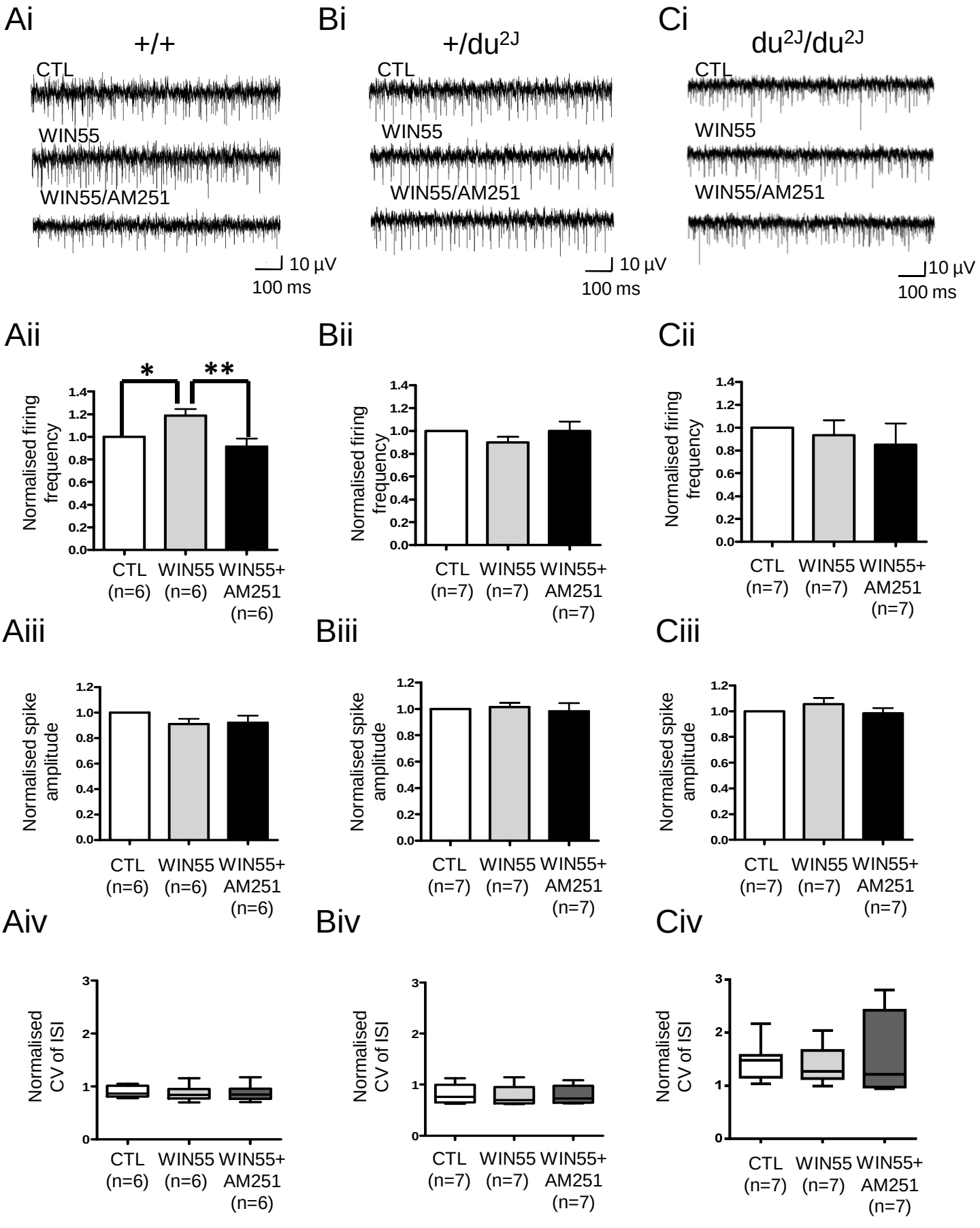

Figure 3. Wang et al

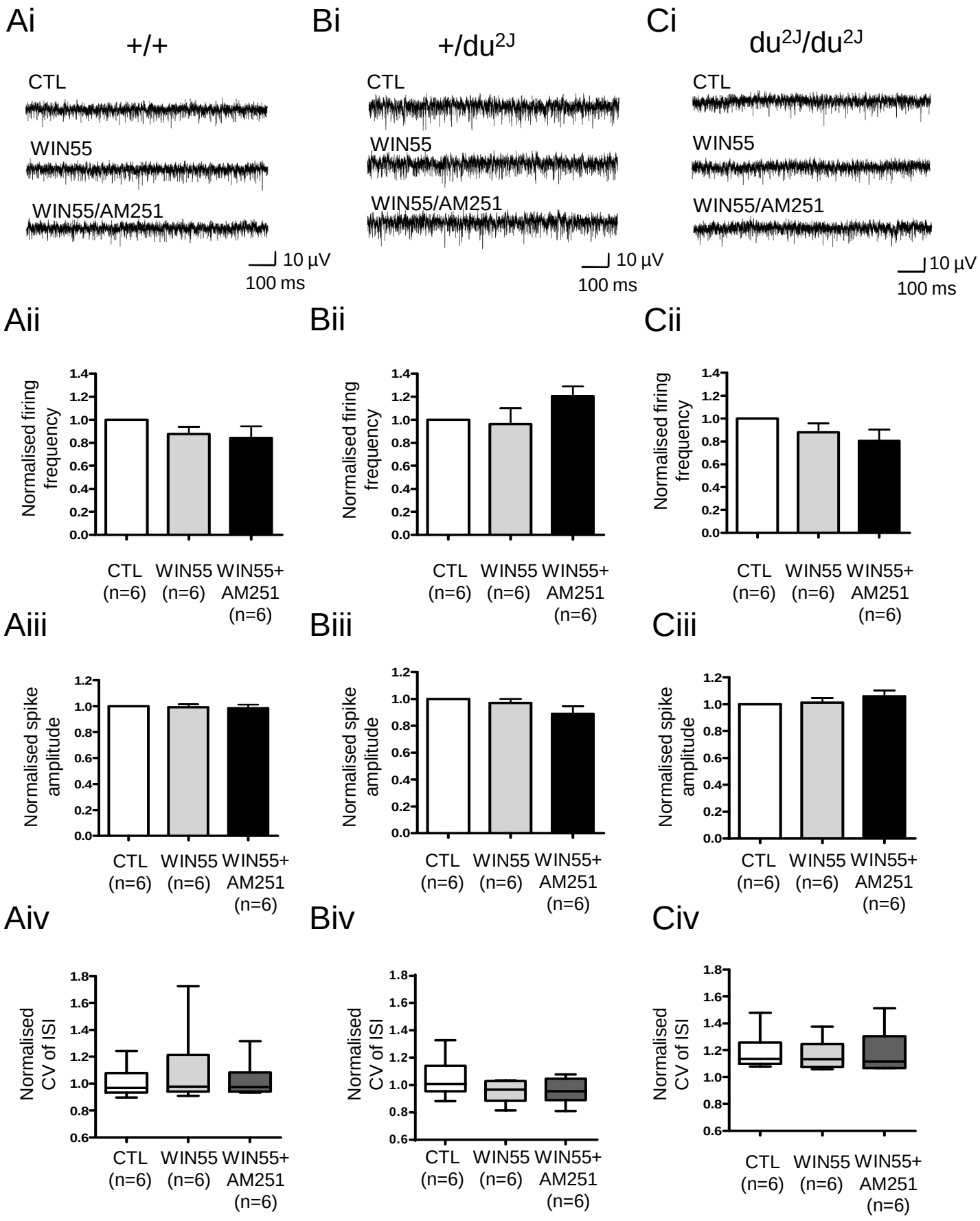

Figure 4. Wang et al

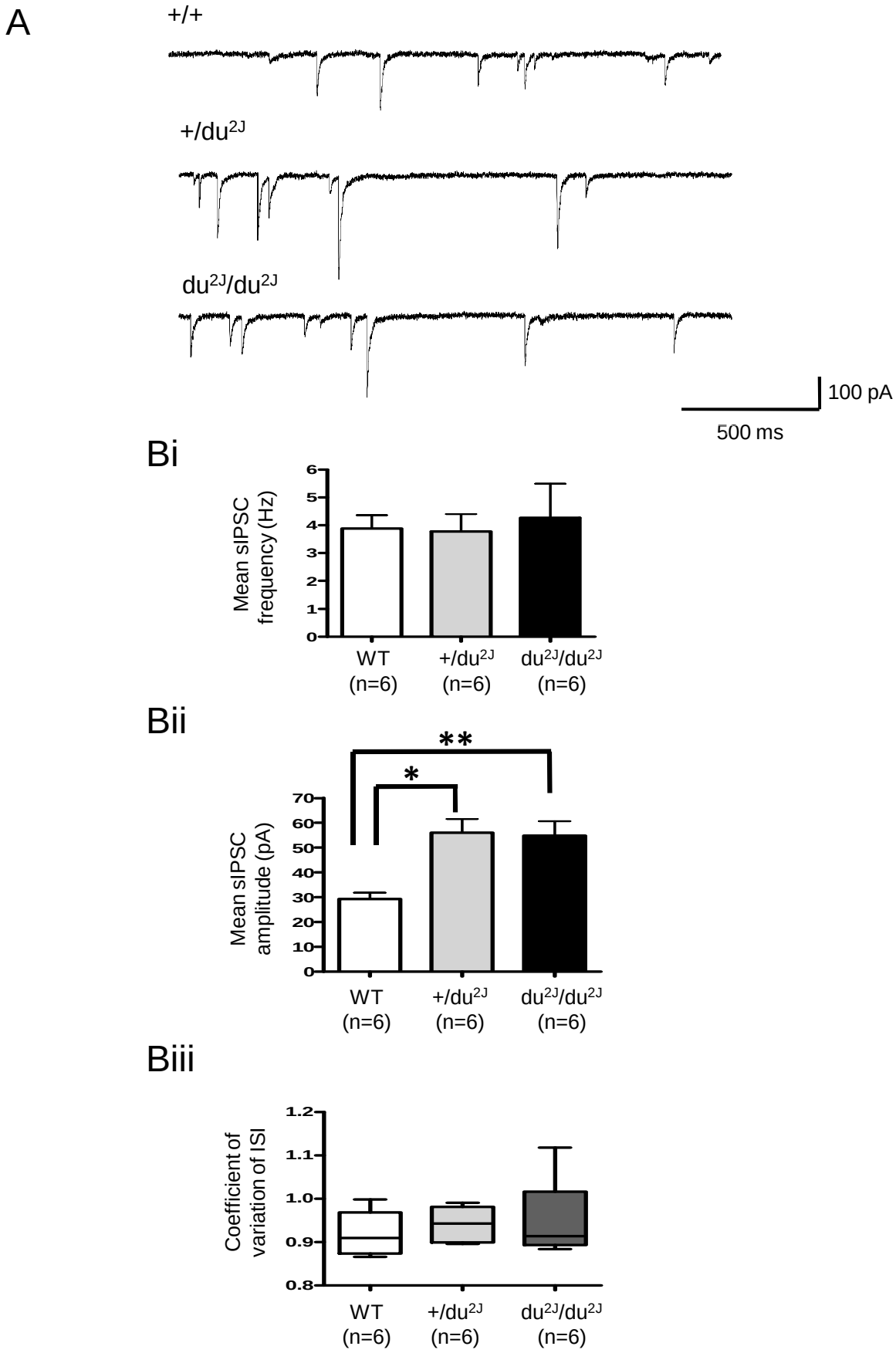

Figure 5. Wang et al

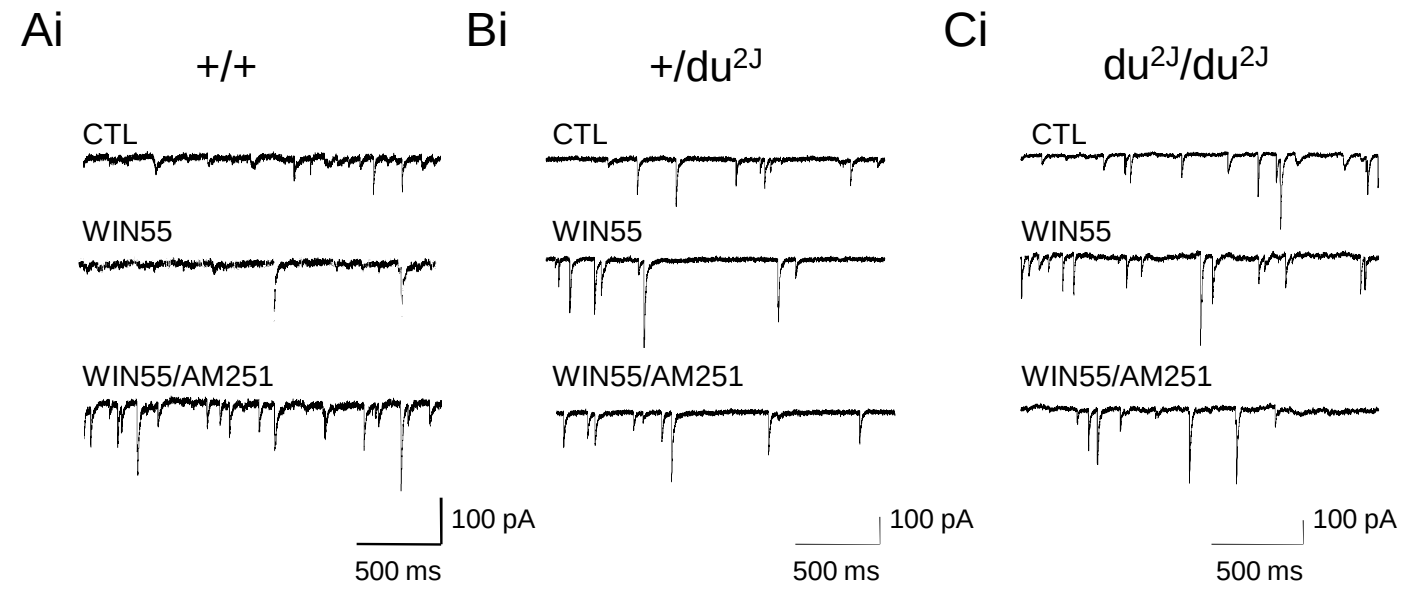

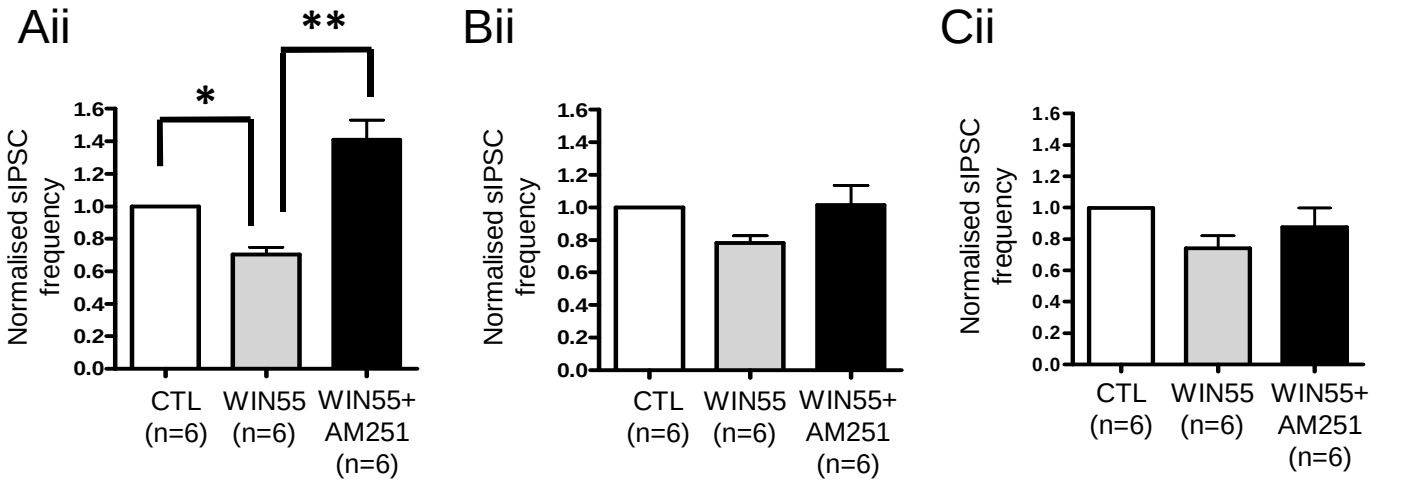

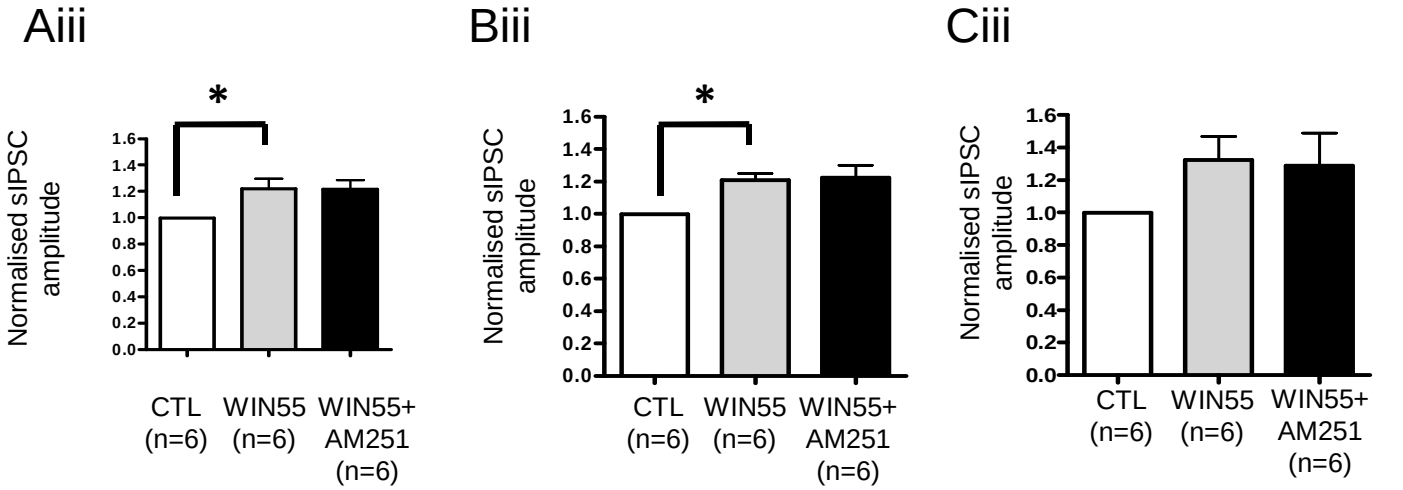

Figure 6. Wang et al

A

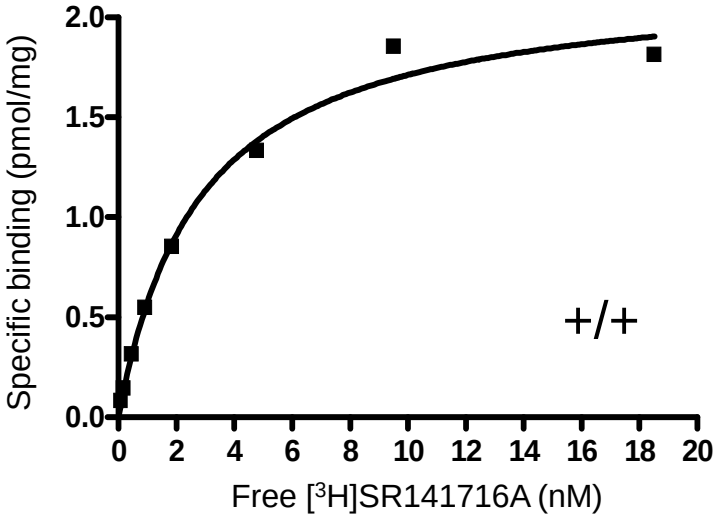

B

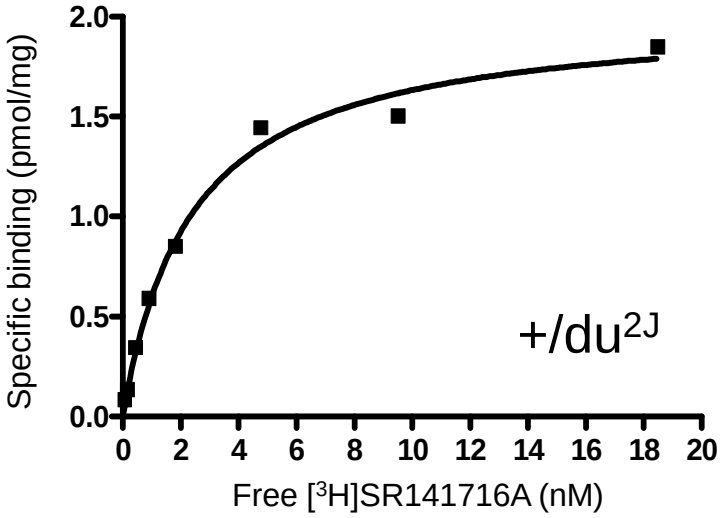

C